Deciphering the Antitoxin-Regulated Bacterial Stress Response via Single-Cell Analysis

Lina Wu,[†,*] Miaomiao Zhang,[†] Yiyi Song,[†] Minfang Deng,[†] Shengbin He,[†] Liuqin Su,[†] Yu Chen,[†] Thomas Keith Wood,[§,] and Xiaomei Yan[†,*]

[†] MOE Key Laboratory of Spectrochemical Analysis & Instrumentation, Key Laboratory for Chemical Biology of Fujian Province, Collaborative Innovation Center of Chemistry for Energy Materials, Department of Chemical Biology, College of Chemistry and Chemical Engineering, Xiamen University, Xiamen, Fujian 361005, People's Republic of China.

[§] Department of Chemical Engineering, Pennsylvania State University, University Park, PA 16802-4400, USA.

* To whom correspondence should be addressed. Phone: 86-592-2184519. E-mail: alina1222@xmu.edu.cn, xmyan@xmu.edu.cn.

ABSTRACT

Bacterial toxin-antitoxin (TA) systems, which are diverse and widespread among prokaryotes, are responsible for tolerance to drugs and environmental stresses. However, the low abundance of toxin and antitoxin proteins renders their quantitative measurement in single bacteria challenging. Employing a laboratory-built nano-flow cytometer (nFCM) to monitor a tetracysteine (TC)-tagged TA system labelled with the biarsenical dye (FlAsH), we here report the development of a sensitive method that enables the detection of basal-level expression of antitoxin. Using the *Escherichia coli* MqsR/MqsA as a model TA system, we reveal for the first time that, under its native promoter and in the absence of environmental stress, there exist two populations of bacteria with high or low levels of antitoxin MqsA. Under environmental stress, such as bile acid stress, heat shock, and amino acid starvation, the two populations of bacteria responded differently in terms of MqsA degradation and production. Subsequently, resumed production of MqsA after amino acid stress was observed for the first time. Taking advantage of the multiparameter capability of nFCM, bacterial growth rate and MqsA production were analyzed simultaneously. We found that under environmental stress, the response of bacterial growth was consistent with MqsA production but with an approximate 60 min lag. Overall, the results of the present study indicate that stochastic elevation of MqsA level facilitates bacterial survival, and the two populations with distinct phenotypes empower bacteria to deal with fluctuating environments. This analytical method will help researchers gain deeper insight into the heterogeneity and fundamental role of TA systems.

Prokaryotic toxin-antitoxin (TA) systems are usually operons consisting of two adjacent genes that encode a stable toxin protein that interferes with vital cell processes such as translation, DNA replication, and cell wall growth and a labile antitoxin that binds to and neutralizes toxin activity.[1,2] Under conditions of environmental stress, unstable antitoxins will be degraded, which can free toxins to inhibit the growth of bacteria or result in a stress-tolerant dormant state (persistence).[3-6] However, the mechanisms regulating their activity and the molecular targets of TA systems remain poorly understood.[2] The increasingly expanding roles of TA systems in mediating antibiotic resistance require ever-increasing efforts to uncover the molecular mechanisms by which TA systems regulate growth and persistence.[5-8]

Most studies of TA systems have been conducted at the transcriptional level (PCR screen, gene chip). For example, mRNA of TA systems has been extracted followed by quantitative real-time reverse-transcription PCR (qRT-PCR), Northern analysis, semi-quantitative primer extension, or microarrays to quantify mRNA levels.[9-12] However, emerging evidence suggests that investigations at the transcriptional level are insufficient for the quantitative description of biological systems.[13] It has been reported that TA systems primarily regulate bacterial metabolism at the protein level. Therefore, focusing only on transcript analysis might lead researchers to overlook some key factors that can cause persistence formation.[14,15] Western blot analysis is the most utilized method for protein expression analysis and has been used to measure TA responses to different

stressors.[9,16] However, TA systems show highly heterogeneous expression among individual cells when bacteria encounter environmental stress, and a specific subpopulation could be responsible for the formation of multidrug resistant persister cells.[17-19] Therefore, it is necessary to develop sensitive and rapid methods of measuring the abundance of TA proteins at the single-cell level so researchers may identify distinct subsets that might be easily masked by ensemble-averaged techniques.

The current approach to confirm and quantify TA expression in individual bacteria is fluorescence microscopy using fluorescent protein fusion with TA systems.[17] However, routine application of microscopy for the investigation of TA systems is hampered due to the tedious procedures and limited statistical power. The high heterogeneity of TA expression and the very low frequency of persister cells (typically 10^{-4} to 10^{-6} of the bacterial population) require rapid detection of a large number of bacterial cells to make data interpretation more conclusive.

Flow cytometry (FCM) is a high-throughput technique for multiparameter single cell analysis. However, the low-level expression of most TA systems in their native state presents a great challenge for conventional flow cytometers.[20] Employing strategies for single-molecule fluorescence detection in a sheathed flow, our laboratory has developed nano-flow cytometry (nFCM).[21,22] Depending on the instrumental setup, the apparatus can be hundreds of times more sensitive in fluorescence detection and hundreds to tens of thousands of times more sensitive in light scattering detection than conventional FCM.[23,24] The detection of bacterial

autofluorescence, low copy number of β-glycosidase, and even single phycoerythrin proteins has been reported.[21,25,26]

The tetracysteine-biarsenical (TC-FlAsH) system is an intelligent strategy developed by Tsien *et al*. for site-specific fluorescent labeling of proteins in live cells.[27,28] The small size of the TC-peptide tag makes it easy to incorporate into the target protein gene and renders minimal interference with protein structure and function.[29,30] Here, we report the development of a sensitive strategy for the quantitative analysis of antitoxin expression in individual bacterial cells based on TC-FlAsH labeling combined with nFCM. Using MqsR/MqsA as a model TA system, two distinct populations of MqsA with high and low production were observed, and the bacterial growth rate was measured simultaneously with MqsA production to study their correlation under different environmental stresses.

RESULTS AND DISCUSSION

Design of the nFCM-TC-FlAsH Strategy for Single-cell Analysis of Antitoxin Production. The principle for single-cell analysis of TA production is depicted in Scheme 1. We selected MqsR/MqsA, an important TA, as the model system. Considering that antitoxin MqsA is the direct regulator of the general stress response, that MqsA is normally produced at a much higher level than toxin MqsR and that MqsA is degraded rapidly under stress conditions,[15,16] we chose to analyze the production of antitoxin MqsA in single bacterial cells. A 12-amino acid TC tag was fused to the C-terminus of MqsA. To mimic the native situation of toxin/antitoxin expression, we constructed the *mqsRA* gene with its native promoter (*pmqsRA*) in a

pCA24N plasmid with deletion of its pT5-*lac* promoter. The recombinant plasmid, pCA24N-*pmqsRA*-*mqsR*-*mqsA*-TC (henceforth pPRAtc), was transformed into BW25113 Δ*mqsRA* ΔKm, which lacks the chromosomal *mqsRA* loci so there is no background expression of the TA system. After the bacterial culture reached an OD_{600} of 0.5 (mid-exponential phase), MqsA-TC was specifically labeled green with a cell-membrane-permeable biarsenical dye FlAsH-EDT_2 (EDT = 1, 2-ethanedithiol) and analyzed by the nFCM. At the same time, the bacterial concentration was measured by counting the events rate with concurrent side scatter and green fluorescence signals. Bacterial growth rate can be derived from the change in bacterial concentration over time. Therefore, both the level of MqsA antitoxin and bacterial growth rate can characterized simultaneously.

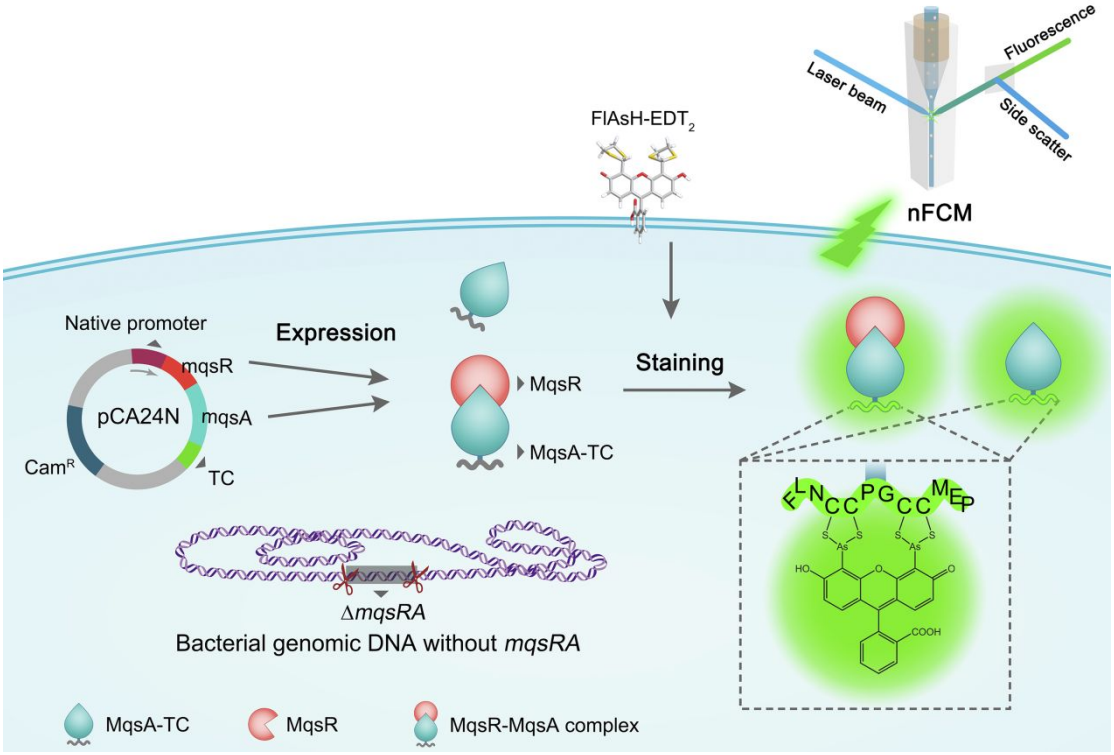

Scheme 1. Schematic of antitoxin MqsA production and the TC-FlAsH labeling strategy for single cell analysis of MqsA by flow cytometry.

Sensitivity and Resolution Evaluation of nFCM Analysis of Antitoxin MqsA Production in Single Bacterial Cells. To evaluate the sensitivity of the proposed nFCM-TC-FlAsH approach, detection of antitoxin MqsA expression under its native promoter was performed. Bacteria were grown in Luria-Bertani (LB) medium for this proof-of-principle experiment. Representative side scatter (SS) and fluorescence (FL) burst traces for BW25113 Δ*mqsRA* ΔKm transformed with plasmid pCA24N-*pmqsRA-mqsR-mqsA* (henceforth pPRA, negative control, no TC tags) and pPRAtc are displayed in Figure 1. Intense SS signals were clearly detected for all the bacterial cells (Figure 1a1, b1). For the fluorescence channel, in contrast to the minimal background fluorescence detected for the negative control, a clear enhancement in peak intensity was observed for pPRAtc transformed cells (Figure 1b2 versus 1a2). Although the production of antitoxin under the native promoter was rather low, a clear right shift in fluorescence burst area was observed on both the bivariate dot-plots (Figure 1c) and the histograms (Figure 1d) when compared to the negative control. The median fluorescence intensities (MFIs) for BW25113 Δ*mqsRA* ΔKm transformed with pPRA or pPRAtc were 340 and 824, respectively. Thus, the expression of antitoxin under its native promoter could be detected in single cells with superior sensitivity.

It has been reported that the expression ratio between toxin and antitoxin can vary by tens to hundreds of fold depending on the module type. For example, antitoxin RelB was estimated to be present in 550–1100 molecules per cell while toxin YdaT might be found in less than 20 molecules per cell.[15,31] After confirming that the nFCM-TC-FlAsH strategy can explicitly detect the MqsA antitoxin in single bacterial cells, the ability to discriminate various antitoxin levels was evaluated. Considering that the expression of TA systems under the native promoter is relatively

low, we used micromolar to millimolar levels of IPTG to induce antitoxin MqsA production in BW25113 Δ*mqsRA* ΔKm transformed with plasmid pCA24N-*plac*-*mqsR*-*mqsA*-TC (henceforth pLRAtc, antitoxin under pT5-*lac* promoter with TC tag). That is, the expression of *mqsR*/*mqsA* could be regulated by a strong pT5-*lac* promoter through IPTG induction. The measured fluorescence burst area distribution histograms are shown in Figure 1e. When the median fluorescence burst area was plotted against the IPTG concentration, an exponential curve was obtained (Figure 1f). At the low micromolar concentration of IPTG, the trend was steep and a small increase in the IPTG concentration led to a significant augmentation in antitoxin production. This increase in fluorescence intensity started to slow down at 1 mM IPTG, then reached a plateau. Clearly, nFCM provides high resolution for the quantitative measurement of low level antitoxin in single bacterial cells.

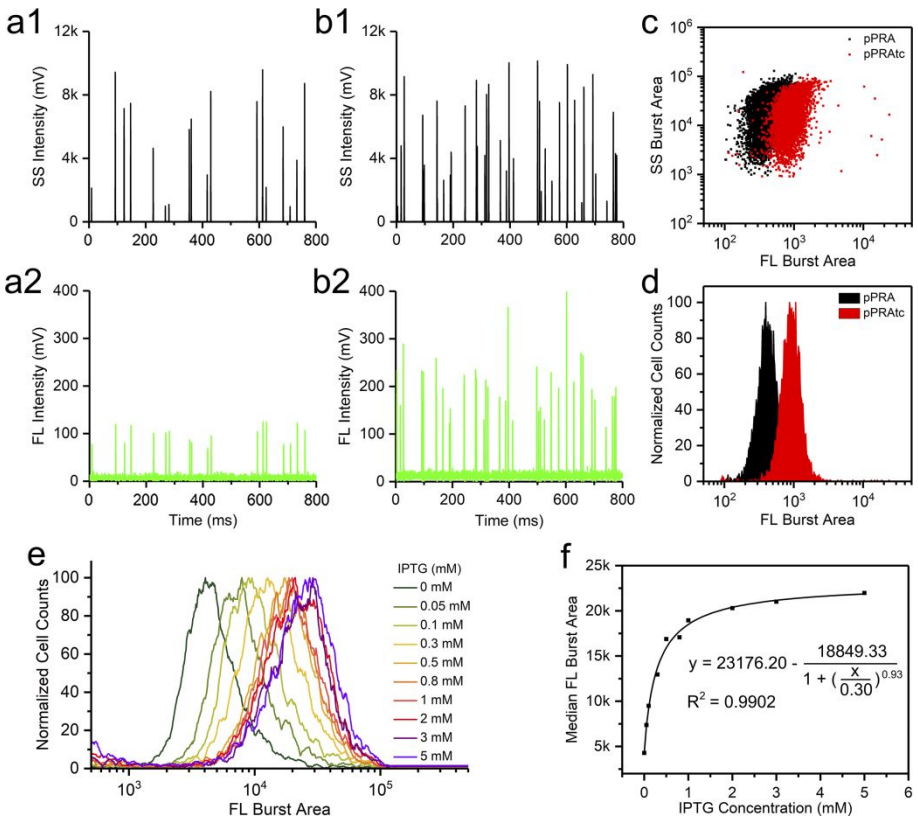

Figure 1. Flow cytometric analysis of antitoxin MqsA using the nFCM-TC-FlAsH strategy. (a and b) Side scatter (SS) and fluorescence (FL) burst traces for BW25113 Δ*mqsRA* ΔKm/pPRA (negative control) (a) and BW25113 Δ*mqsRA* ΔKm/pPRAtc (b). (c and d) Bivariate dot-plots of side scatter burst area versus fluorescence burst area (c) and histograms of fluorescence burst area distribution (d) for BW25113 Δ*mqsRA* ΔKm/pPRA (black) and BW25113 Δ*mqsRA* ΔKm/pPRAtc (red). (e) Histograms of fluorescence burst area distribution for BW25113 Δ*mqsRA* ΔKm/pLRAtc induced with 0, 0.05, 0.1, 0.3, 0.5, 0.8, 1, 2, 3, and 5 mM IPTG. The histograms were normalized to facilitate an easy comparison. (f) Dose response curve of MqsA production in single bacterial cells at various IPTG concentrations.

Simultaneous Measurement of Antitoxin Production and Bacterial Growth under Various Stresses. TA systems are "stress managers" that are essential to the mediation of general stress response (GSR).[16,32] The GSR enables cells to survive long periods of starvation or other environmental stresses.[32] To study the relationship between the production of antitoxin and bacterial growth, the nFCM-TA-FlAsH strategy was applied for the analysis under conditions of bile acid stress, heat shock, and amino acid starvation. Bacteria were grown in M9 minimal medium instead of LB medium for all the stress experiments to reduce the influence of osmolytes and other unknown compounds present in yeast extract of LB medium. Meanwhile, the effect of FlAsH staining and BAL washing on bacterial growth was confirmed to be negligible (Supplementary Figure S1).

1. Bile Acid Stress Degrades MqsA and Triggers Cell Growth Cessation

with a 60-min Lag. Bile acid stress can cause lipid peroxidation and induce oxidative stress response.[33] The MqsR/MqsA system is a multi-faceted regulator that not only facilitates the growth of *E. coli* populations in human gastrointestinal tract through decreased metabolism, but also improves deoxycholate tolerance when exposed to bile acid stress.[16,33] Bile acid stress experiments were performed by treating BW25113 Δ*mqsRA* ΔKm/pPRAtc with or without (normal conditions) 4.5% NaDC. BW25113 Δ*mqsRA* ΔKm/pPRA without the TC-tag serves the blank control (Figure 2a BC). Bacteria were sampled at 0, 5, 30, 60, 90, 120, and 180 min after stress induction. Figure 2a(i)–(vii) shows the bivariate dot-plots of MqsA production versus side scatter of BW25113 Δ*mqsRA* ΔKm/pPRAtc treated with (Figure 2a2) or without (Figure 2a1) NaDC. Unlike the single population of MqsA production in LB medium cultivation (Figure 1c), under the normal conditions in M9 minimal medium cultivation, two populations of bacteria with high and low levels of MqsA production were observed at all time points, and most cells (around 90%) exhibit low levels of MqsA (Figure 2a1, 2b1). From 0 to 180 min, the MFI of the populations with high or low levels of MqsA production grew from 1888 to 4018 and from 425 to 698, respectively. These results indicate that, under the normal conditions, MqsA production is heterogeneous and increases in both the low- and high-level populations during the logarithmic phase. Note that the different levels of MqsA production for bacteria cultured in M9 medium is not due to the plasmid copy number (Supplementary Figure S2, S3 and Table S1).

Under bile acid stress, the population with high level of MqsA production

disappeared immediately upon addition of NaDC (Figure 2a2(ii)–(vii), 2b2), whereas the signal of the population with low level of MqsA production remained constant. These data suggest that, under bile acid stress, only the population with a high level of MqsA was degraded while the population with a low level of MqsA remained undisturbed. Figure 2c shows the variation of MFI of total MqsA production versus the exposure time under both the normal conditions and upon NaDC treatment. Note that the signal of blank control (Supplementary Figure S4 for all of the blank control data) was subtracted, i.e., ($MFI_{PRAtc,\ NaDC}$–MFI_{PRA}) or ($MFI_{PRAtc,\ Normal}$–MFI_{PRA}). Clearly, MqsA production decreased immediately after the onset of bile stress and then remained at a relatively constant low level. However, under normal conditions, the signal of total MqsA production started to grow at 5 min and continued to increase, with a 3.9-fold enhancement observed at 180 min.

Regarding the bacterial growth rate measured at the same time, despite the immediate degradation of MqsA at 5 min, bacterial growth arrest did not occur until 60 min after induction of the stress. Fluorescence microscopic examination was conducted in parallel and the micrograph of the blank control (Figure 2d BC) showed almost no fluorescence signal. Figure 2d(i)–(iv) shows the fluorescence micrographs of BW25113 Δ*mqsRA* ΔKm/pPRAtc under normal growth conditions (Figure 2d1) and bile acid stress (Figure 2d2) for 0, 5, 60, and 120 min. In agreement with the results obtained by nFCM, microscopic analysis revealed an increased fluorescence of bacteria over cultivation time under normal conditions. When the bile acid stress was induced, the intensity of the bacterial fluorescence decreased immediately and

markedly. The number of bacteria with bright fluorescence started to decrease in as short as 5 min. Taking advantage of the superior resolution of nFCM, two populations of bacteria with low or high levels of MqsA and their different responses to bile acid stress were observed for the first time.

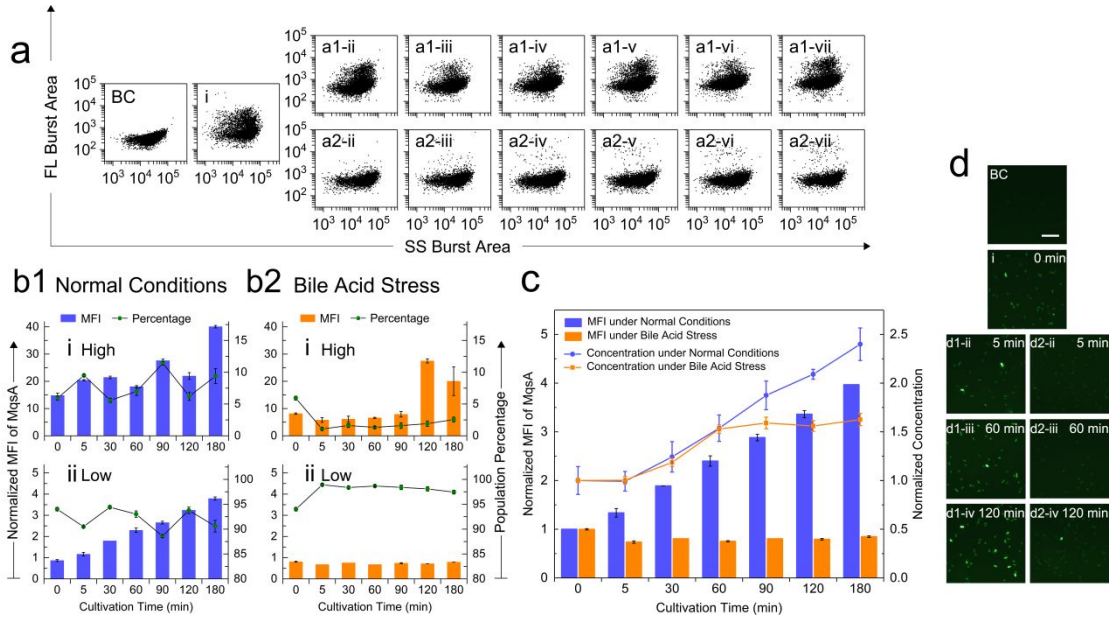

Figure 2. Simultaneous detection of MqsA production (under its native promoter) and bacterial growth upon induction of bile acid stress. (a) Bivariate dot-plots of MqsA-TC-FlAsH fluorescence burst area versus SSC burst area for BW25113 Δ*mqsRA* ΔKm/pPRAtc with (a2(ii)–(vii)) or without (a(i), a1(ii)–(vii)) 4.5% NaDC treatment for 0, 5, 30, 60, 90, 120, and 180 min. (b) High and low MqsA production levels (bar graph) and population percentage (line chart) versus the exposure time upon treatment with and without NaDC. (c) Temporal MqsA antitoxin production (bar graph) and bacterial concentration (line chart) of BW25113 Δ*mqsRA* ΔKm/pPRAtc upon treatment with and without NaDC. (d) Fluorescence microscopy images show the production of MqsA in BW25113 Δ*mqsRA* ΔKm/pPRAtc cultivated with (d2(ii)–(iv)) or without (d(i), d1(ii)–(iv)) NaDC treatment at 0, 5, 60, and 120 min. Scale bar: 5 μm. (BC) is the blank control

(BC) where the TC-tag is absent (BW25113 Δ*mqsRA* ΔKm/pPRA). The error bar in b) and c) represents the standard deviation of three replicates.

2. Heat Shock Upregulates MqsA Production Only in the Population of Low Abundance and Is Accompanied by Continued Bacterial Growth. Heat shock response is an important protective mechanism that is crucial to bacterial survival and adaptation to hostile environmental conditions. Regulation of MqsA production during heat shock was evaluated using nFCM-TC-FlAsH analysis of individual cells (Figure 3). Experiments were conducted by transferring cells from 37°C to 42°C at an OD_{600} of 0.5. Cells of BW25113 Δ*mqsRA* ΔKm/pPRAtc grown at a constant temperature of 37°C (the normal conditions) served as a negative control. In contrast to bile acid stress, the two populations of bacteria with high and low levels of MqsA production remained observable throughout the entire process of heat stress, which resembles what happens under the normal conditions (Figure 3a, and Figure 2a1). By plotting the signal for heat stress ($MFI_{PRAtc,\ Heat}$-MFI_{PRA}) and the normal conditions against the duration of stress, it was determined that upon heat stress, the production of MqsA continued to increase over time and the rate of increasing was even higher than that of the normal conditions (Figure 3c). After 3 h of heat stress, the fluorescent signal of MqsA was 1.2-fold higher than that of the normal conditions, and 4.5-fold higher than prior to the heat shock. This increase in MqsA levels was in accordance with the fact that Lon, the antitoxin-degrading protease, does not increase during heat shock.[34] The increased production of MqsA under heat shock indicates that bacterial growth was not arrested. As expected, there was a continuous growing trend in

bacterial concentration under heat stress, and the growth rate was only slightly slower than that of the normal conditions. As shown in Figure 3a/b, we note that, as heat shock continues, the increase of MqsA production occurred only in the bacterial population of low MqsA abundance whereas the fluorescent signal in the population of a high level of production remained almost unchanged. Consistent with data collected using nFCM, the results of microscopic analysis (Figure 3d) showed an increase in fluorescence intensity for bacteria grown at 42°C, while the brightness of the small amount bacteria with high fluorescence had intensity similar to those prior to heat shock.

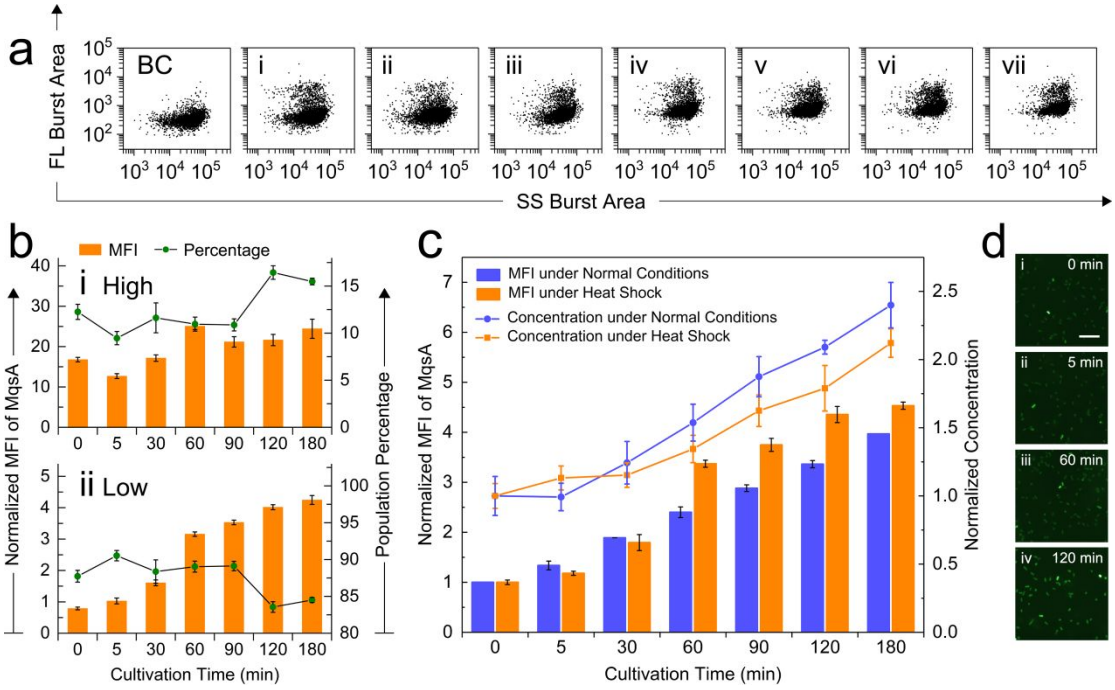

Figure 3. Simultaneous detection of MqsA production and bacterial growth upon heat shock. (a)/(d) Bivariate dot-plots of MqsA-TC-FlAsH fluorescence burst area versus SSC burst area (a) and fluorescence micrographs (d) for BW25113 Δ*mqsRA* ΔKm/pPRAtc cultured at 42°C. Scale bar: 5 μm. (b) High and low MqsA production levels (bar graph) and population percentage (line

chart) versus the exposure time upon treatment at 42°C. (c) Temporal MqsA antitoxin production (bar graph) and bacterial growth (line chart) of BW25113 Δ*mqsRA* ΔKm/pPRAtc cultured at 42°C or 37°C. The error bar in b) and c) represents the standard deviation of three replicates.

3. MqsA Is Degraded and Regenerated upon Amino Acid Starvation. *E. coli* encodes at least 39 TA loci, and expression of many of these can be induced by amino acid starvation (AA starvation).[10,33] Figure 4 shows the results obtained upon serine starvation stress by adding 2.0 mg/mL DL-serine hydroxamate (SHX). Unlike bile acid stress, the population of bacteria with a high level of MqsA did not disappear, similar to the response to heat shock (Figure 4a). By plotting the signal for serine starvation stress ($MFI_{PRAtc,\ SHX}$-MFI_{PRA}) and normal conditions against the duration of stress, we found that MqsA was degraded to about 25% of the pre-starvation level within 5 min under serine starvation (Figure 4c). However, a rebound of MqsA production was observed at 30 min and reached a steady state around 90 min. At 180 min, the signal increased to 160% of the pre-starvation level, though it was only one-third of that observed under normal conditions. Similarly, using western blot analysis and the strong pT7-*lac* promoter, Gerdes *et al*. observed an initial decrease in antitoxin RelB at 30 min followed by an increase in production at 180 min to a steady-state post starvation level, which was 60% that of the pre-starvation level.[9] The bacteria growth measured simultaneously with MqsA production continued under serine starvation within 60 min, after which it was arrested, consistent with the degradation of MqsA at 5 min, which is similar to the results observed for bile acid stress. Interestingly, after 90 min,

the growth arrest was depressed and regrowth began in accordance with the regeneration of MqsA at 30 min. Both the arrest and regrowth showed a 60 min-lag compared with MqsA degradation or regeneration. When combined with the previous results, these findings confirm that MqsA has a rapid response to environmental stress whereas the response of bacterial growth showed a 60 min delay. Fluorescence micrographs (Figure 4d) showed similar trends in fluorescence intensity as indicated by nFCM. The fluorescence intensity of bacteria decreased at 5 min and increased at 60 and 120 min.

Amino acid starvation was also conducted with isoleucine starvation and similar result was observed (Supplementary Figure S5): MqsA was degraded and regenerated quickly under AA starvation. We speculate that the regeneration of MqsA may indicate the bacteria's adaptation to stressful environment. It should be noted that this is the first report of MqsA regeneration in response to serine starvation and the first to report the same response was found toward isoleucine starvation.

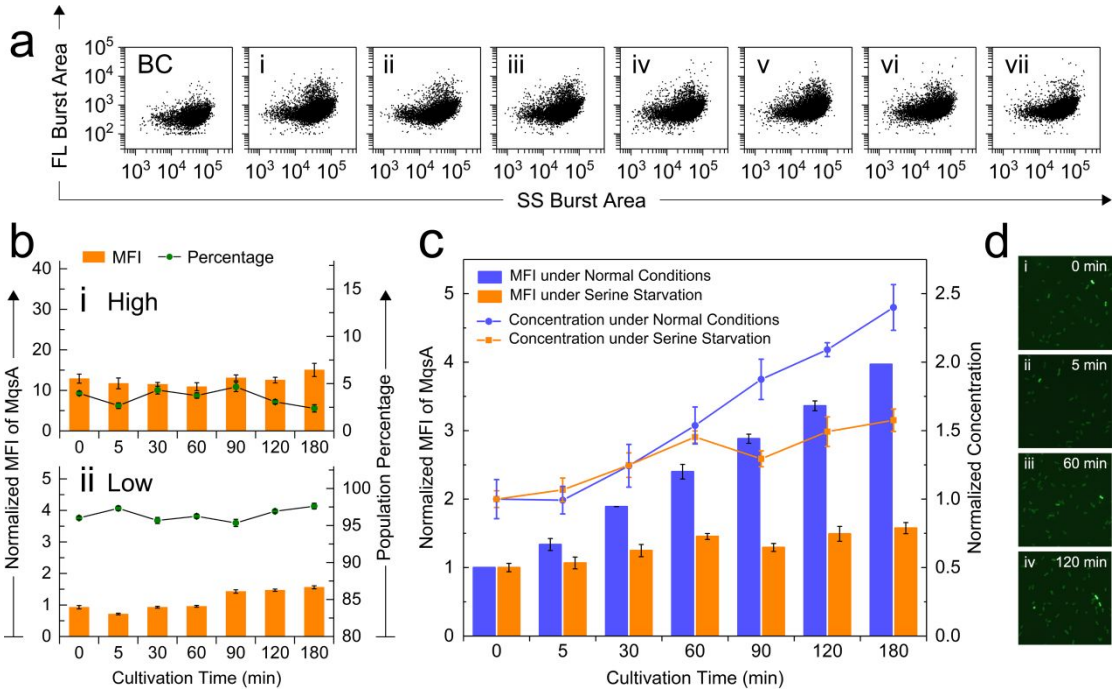

Figure 4. Simultaneous detection of MqsA production and bacterial growth upon serine starvation. (a)/(d) Bivariate dot-plots of MqsA-TC-FlAsH fluorescence burst area versus SSC burst area (a) and fluorescence micrographs (d) for BW25113 Δ*mqsRA* ΔKm/pPRAtc with 2.0 mg/mL SHX treatment. Scale bar: 5 μm. (b) High and low MqsA production levels (bar graph) and population percentage (line chart) versus the exposure time upon treatment with and without SHX. (c) Temporal MqsA antitoxin production (bar graph) and bacterial growth (line chart) of BW25113 Δ*mqsRA* ΔKm/pPRAtc upon treatment with and without SHX. The error bar in b) and c) represents the standard deviation of three replicates.

CONCLUSIONS

Single-cell analysis of how bacteria make use of antitoxins to regulate the bacterial stress response is essential for the mechanistic understanding of TA systems. Combining TC-FlAsH with nFCM, we developed an ultrasensitive and rapid method for the quantitative detection of antitoxin levels in individual bacteria and discovered

that MqsA rapidly responds to different environmental stresses. Specifically, we observed MqsA degradation upon bile acid stress, production upon heat stress, and degradation followed by regeneration upon amino acid starvation. Through simultaneous evaluation of bacterial growth by nFCM, we found that bacterial growth responses were consistent with MqsA production, but with a lag of about 60 min. Based on insights gained by studying the stress response with the MqsR/MqsA system, we found that nutrient limitation is a stress that can be self-healed by bacteria after suspending both growth and protein synthesis. Furthermore, two populations of bacteria with high and low level of MqsA production were observed in the absence of environmental stress, and the population with a high level of MqsA production disappeared under stress conditions that resulted in bacterial growth arrest.

Stochastic TA expression offers the opportunity to generate long-term heterogeneity in a clonal population for implementing a bet-hedging strategy,[17,35] whereas stochastic activation of the toxin leads to the formation of dormant persisters.[17,36] The switch between normal and persistent phenotypes can be driven by proteolysis of the antitoxin, stochastic fluctuation, or a change in the growth rate.[37] Hence, we posit that heterogeneous production of MqsA may be another strategy for helping bacteria to survive, which results in bacterial phenotypes being switched. Our high-throughput technique of nFCM-TC-FlAsH provides an advanced means to decipher the heterogeneous populations of antitoxins and enables the investigation of TA systems at the protein level, which is highly desirable for elucidating the physiological role of TA systems and promoting the development of TA-related

research. However, further investigation is needed to simultaneously investigate both toxins and antitoxins at the single-cell level. TC tags could be combined with other fluorophores for dual fluorescent labeling of toxins and antitoxins.

METHODS

Reagents and Chemicals. The TC-FlAsH In-Cell Tetracysteine Tag Detection Kit was purchased from Molecular Probes of Invitrogen, Inc. (Eugene, OR, USA). DL-serine hydroxamate (SHX) and DL-valine were bought from Sigma (St. Louis, MO, USA). Sodium deoxycholate (NaDC), isopropyl β-D-1-thiogalactopyranoside (IPTG), tryptone, yeast extract, and agar were acquired from Sangon Biotech (Shanghai, China). Other reagents were purchased from Sinopharm Chemical Reagent (Shanghai, China). Ultrapure water prepared using a Milli-Q RG unit was used in all experiments (Millipore, Bedford, MA, USA).

Bacterial Strains and Plasmid Construction. *E. coli* DH5α was used for all the cloning experiments. Plasmid pCA24N-*pmqsRA*-*mqsR*-*mqsA*-TC (henceforth pPRAtc) was constructed by inserting the native promoter *pmqsRA*, toxin open reading frame (*mqsR*), and antitoxin open reading frame labeled with TC tag (*mqsA*-*TC*) into the pCA24N at the *Xho*I/*Pst*I sites. Plasmid pCA24N-*pmqsRA*-*mqsR*-*mqsA* (henceforth pPRA) without the MqsA TC tag was constructed in the same way. Plasmid pCA24N-*mqsR*-*mqsA*-TC (henceforth pLRAtc) was constructed by inserting the *mqsR* and *mqsA*-TC into the pCA24N at the *Sal*I/*Pst*I sites behind the pT5-*lac* promoter site. All the constructed plasmids were verified by sequencing. *E. coli* K-12 BW25113 Δ*mqsRA* ΔKm transformed with pPRAtc, pLRAtc, and pPRA was used for the following experiments.

Bacterial Cell Culturing. BW25113 Δ*mqsRA* ΔKm/pPRAtc, BW25113 Δ*mqsRA* ΔKm/pLRAtc, and BW25113 Δ*mqsRA* ΔKm/pPRA were grown in either Luria-Bertani (LB) medium (10 g tryptone, 5 g yeast extract, and 10 g NaCl per liter) or M9 minimal medium (12.8 g $Na_2HPO_4 \cdot 7H_2O$, 3.0 g KH_2PO_4, 0.5 g NaCl, 1.0 g NH_4Cl, 2 mL 1 M $MgSO_4$, 0.1 mL 1 M $CaCl_2$, 0.4% D-glucose per liter) containing 30 μg/mL chloramphenicol to retain the plasmids. Bacteria were incubated to the exponential growth phase at 37°C in baffled flasks on a 250 rpm rotary shaker. To obtain different amounts of MqsA antitoxin protein, BW25113 Δ*mqsRA* ΔKm/pLRAtc (with an OD_{600} of 0.5) was induced by exposure to 0, 0.05, 0.1, 0.3, 0.5, 0.8, 1, 2, 3, and 5 mM IPTG for 3 h.

FlAsH Staining. When the bacteria reached the exponential phase (with an OD_{600} of 0.5), 20 μL of bacterial solution was preloaded with 5 μM FlAsH-EDT_2 and incubated at 37°C in the dark for 3 h with shaking (250 rpm). The mixture was centrifuged (8,000 g, 5 min, 4°C) and washed twice with 50 μL phosphate-buffered saline (PBS) containing 0.5 mM 2,3-dimercaptopropanol (BAL). The bacterial cells were suspended in 50 μL of PBS for flow cytometric analysis.

Stress Response. When BW25113 Δ*mqsRA* ΔKm/pPRAtc and BW25113 Δ*mqsRA* ΔKm/pPRA were grown exponentially (with an OD_{600} of 0.25), 20 μL of each bacterial solution was preloaded with 5 μM FlAsH-EDT_2, and incubated at 37°C in the dark for 3 h with shaking (250 rpm). All of the stress conditions were induced at an OD_{600} of 0.5. The bacteria were stressed by NaDC (45 mg/mL) for the bile acid stress response experiment, DL-serine hydroxamate (SHX, 2.0 mg/mL) for serine starvation, and DL-valine (0.5 mg/mL) for isoleucine starvation. Heat shock was induced by transferring bacteria from 37°C to 42°C. Cells of BW25113 Δ*mqsRA*

ΔKm/pPRAtc were cultivated without the stressor at 37°C (normal growth conditions) as negative controls. Samples were taken after the stress conditions at 0 (before medicine treatment), 5, 30, 60, 90, 120, and 180 min in the dark for 3 h with shaking (250 rpm). The mixture was centrifuged (8,000 g, 5 min, 4°C) and washed twice with 50 μL PBS containing 0.5 mM BAL. The bacterial cells were suspended in 70 μL or 5 μL of PBS for flow cytometric or fluorescence microscopic analysis, respectively.

Flow Cytometry and Fluorescence Microscopy Analysis. FlAsH-labeled samples were analyzed with a laboratory-built nFCM equipped with a solid-state 488 nm CW laser as the excitation source. The light emitted from individual bacteria was collected using a microscopic objective and then directed by a dichroic beam splitter into two light paths for side scatter and green fluorescence (520/35) detection by two PMT detectors, respectively. For each bacterial sample, a data acquisition time of 180 s was used. Fluorescence images were generated using an IX73 fluorescence microscope (Olympus) equipped with a U plan Semi Apochromat objective 100×/1.3, WD 0.2 (spring, oil) oil-immersion objective lens.

ASSOCIATED CONTENT

Supporting Information

Supplementary Figures 1 to 5 and Table S1 (PDF)

AUTHOR INFORMATION

Corresponding Author

*E-mail: alina1222@xmu.edu.cn

*E-mail: xmyan@xmu.edu.cn

ORCID

Lina Wu: 0000-0002-7106-4752

Xiaomei Yan: 0000-0002-7482-6863

Conflict of interest

X.Y. declares competing financial interests as a cofounder of NanoFCM Inc., a company committed to commercializing the nano-flow cytometry (nFCM) technology.

ACKNOWLEDGMENTS

This work was supported by the National Natural Science Foundation of China (21877091, 21472158, 21627811, 21475112 and 21521004); the Fundamental Research Funds for the Central Universities (20720160028); and the Natural Science Foundation of Fujian Province, China (2016J01076); the NFFTBS (No. J1310024)

REFERENCES

(1) Harms, A., Brodersen, D. E., Mitarai, N., and Gerdes, K. (2018) Toxins, targets, and triggers: an overview of toxin-antitoxin biology. *Mol. Cell 70*, 768-784.

(2) Hall, A. M., Gollan, B., and Helaine, S. (2017) Toxin-antitoxin systems: reversible toxicity. *Curr. Opin. Microbiol. 36*, 102-110.

(3) Page, R., and Peti, W. (2016) Toxin-antitoxin systems in bacterial growth arrest and persistence. *Nat. Chem. Biol. 12*, 208-214.

(4) Yang, Q. E., and Walsh, T. R. (2017) Toxin-antitoxin systems and their role in disseminating and maintaining antimicrobial resistance. *FEMS Microbiol. Rev. 41*, 343-353.

(5) Levin-Reisman, I., Ronin, I., Gefen, O., Braniss, I., Shoresh, N., and Balaban, N. Q. (2017) Antibiotic tolerance facilitates the evolution of resistance. *Science 355*, 826-830.

(6) Harms, A., Maisonneuve, E., and Gerdes, K. (2016) Mechanisms of bacterial persistence during stress and antibiotic exposure. *Science 354*, aaf4268.

(7) Rocker, A., Peschke, M., Kittilä, T., Sakson, R., Brieke, C., and Meinhart, A. (2018) The ng_ζ1 toxin of the gonococcal epsilon/zeta toxin/antitoxin system drains precursors for cell wall synthesis. *Nat. Commun. 9*, 1686.

(8) Piscotta, F. J., Jeffrey, P. D., and Link, A. J. (2019) ParST is a widespread toxin-antitoxin module that targets nucleotide metabolism. *Proc. Natl. Acad. Sci. U. S. A. 116*, 826-834.

(9) Christensen, S. K., Mikkelsen, M., Pedersen, K., and Gerdes, K. (2001) RelE, a global inhibitor of translation, is activated during nutritional stress. *Proc. Natl. Acad. Sci. U. S. A. 98*, 14328-14333.

(10) Christensen-Dalsgaard, M., Jørgensen, M. G., and Gerdes, K. (2010) Three new RelE-homologous

mRNA interferases of *Escherichia coli* differentially induced by environmental stresses. *Mol. Microbiol. 75*, 333-348.

(11) McKenzie, J. L., Robson, J., Berney, M., Smith, T. C., Ruthe, A., Gardner, P. P., Arcus, V. L., and Cook, G. M. (2012) A VapBC toxin-antitoxin module is a posttranscriptional regulator of metabolic flux in mycobacteria. *J. Bacteriol. 194*, 2189-2204.

(12) Ramisetty, B. C., Ghosh, D., Roy Chowdhury, M., and Santhosh, R. S. (2016) What is the link between stringent response, endoribonuclease encoding type II toxin-antitoxin systems and persistence? *Front. Microbiol. 7*, 1882.

(13) de Sousa Abreu, R., Penalva, L. O., Marcotte, E. M., and Vogel, C. (2009) Global signatures of protein and mRNA expression levels. *Mol. Biosyst. 5*, 1512-1526.

(14) Shah, D., Zhang, Z. G., Khodursky, A., Kaldalu, N., Kurg, K., and Lewis, K. (2006) Persisters: a distinct physiological state of *E. coli*. *BMC Microbiol. 6*, 53.

(15) Li, G. W., Burkhardt, D., Gross, C., and Weissman, J. S. (2014) Quantifying absolute protein synthesis rates reveals principles underlying allocation of cellular resources. *Cell 157*, 624-635.

(16) Wang, X. X., Kim, Y., Hong, S. H., Ma, Q., Brown, B. L., Pu, M., Tarone, A. M., Benedik, M. J., Peti, W., Page, R., and Wood, T. K. (2011) Antitoxin MqsA helps mediate the bacterial general stress response. *Nat. Chem. Biol. 7*, 359-366.

(17) Rotem, E., Loinger, A., Ronin, I., Levin-Reisman, I., Gabay, C., Shoresh, N., Biham, O., and Balaban, N. Q. (2010) Regulation of phenotypic variability by a threshold-based mechanism underlies bacterial persistence. *Proc. Natl. Acad. Sci. U. S. A. 107*, 12541-12546.

(18) Tripathi, A., Dewan, P. C., Siddique, S. A., and Varadarajan, R. (2014) MazF-induced growth inhibition and persister generation in *Escherichia coli*. *J. Biol. Chem. 289*, 4191-4205.

(19) Nikolic, N., Didara, Z., and Moll, I. (2017) MazF activation promotes translational heterogeneity of the *grcA* mRNA in *Escherichia coli* populations. *PeerJ 5*, e3830.

(20) Schumacher, M. A., Balani, P., Min, J., Chinnam, N. B., Hansen, S., Vulić, M., Lewis, K., and Brennan, R. G. (2015) HipBA-promoter structures reveal the basis of heritable multidrug tolerance. *Nature 524*, 59-64.

(21) Yang, L. L., Zhu, S. B., Hang, W., Wu, L. N., and Yan, X. M. (2009) Development of an ultrasensitive dual-channel flow cytometer for the individual analysis of nanosized particles and biomolecules. *Anal. Chem. 81*, 2555-2563.

(22) Zhu, S. B., Yang, L. L., Long, Y., Gao, M., Huang, T. X., Hang, W., and Yan, X. M. (2010) Size differentiation and absolute quantification of gold nanoparticles via single particle detection with a laboratory-built high-sensitivity flow cytometer. *J. Am. Chem. Soc. 132*, 12176-12178.

(23) Ma, L., Zhu, S. B., Tian, Y., Zhang, W. Q., Wang, S., Chen, C. X., Wu, L. N., and Yan, X. M. (2016) Label-free analysis of single viruses with a resolution comparable to that of electron microscopy and the throughput of flow cytometry. *Angew. Chem. Int. Ed. 55*, 10239-10243.

(24) Tian, Y., Ma, L., Gong, M. F., Su, G. Q., Zhu, S. B., Zhang, W. Q., Wang, S., Li, Z. B., Chen, C. X., Li, L. H., Wu, L. N., and Yan, X. M. (2018) Protein profiling and sizing of extracellular vesicles from colorectal cancer patients *via* flow cytometry. *Acs Nano 12*, 671-680.

(25) Yang, L. L., Huang, T. X., Zhu, S. B., Zhou, Y. X., Jiang, Y. B., Wang, S., Chen, Y. Q., Wu, L. N., and Yan, X. M. (2013) High-throughput single-cell analysis of low copy number β-galactosidase by a laboratory-built high-sensitivity flow cytometer. *Biosens. Bioelectron. 48*, 49-55.

(26) Yang, L. L., Zhou, Y. X., Zhu, S. B., Huang, T. X., Wu, L. N., and Yan, X. M. (2012) Detection and quantification of bacterial autofluorescence at the single-cell level by a laboratory-built

high-sensitivity flow cytometer. *Anal. Chem. 84*, 1526-1532.

(27) Hoffmann, C., Gaietta, G., Zürn, A., Adams, S. R., Terrillon, S., Ellisman, M. H., Tsien, R. Y., and Lohse, M. J. (2010) Fluorescent labeling of tetracysteine-tagged proteins in intact cells. *Nat. Protoc. 5*, 1666-1677.

(28) Adams, S. R., Campbell, R. E., Gross, L. A., Martin, B. R., Walkup, G. K., Yao, Y., Llopis, J., and Tsien, R. Y. (2002) New biarsenical ligands and tetracysteine motifs for protein labeling in vitro and in vivo: synthesis and biological applications. *J. Am. Chem. Soc. 124*, 6063-6076.

(29) Wu, L. N., Huang, T. T., Yang, L. L., Pan, J. B., Zhu, S. B., and Yan, X. M. (2011) Sensitive and selective bacterial detection using tetracysteine-tagged phages in conjunction with biarsenical dye. *Angew. Chem. Int. Ed. 50*, 5873-5877.

(30) Hecht, K. A., Xiong, Y. J., Barrack, D. A., Ford, N. R., Roesijadi, G., and Squier, T. C. (2018) Distance-matched tagging sequence optimizes live-cell protein labeling by a biarsenical fluorescent reagent AsCy3_E. *ACS Omega 3*, 2104-2110.

(31) Overgaard, M., Borch, J., and Gerdes, K. (2009) RelB and RelE of *Escherichia coli* form a tight complex that represses transcription via the ribbon-helix-helix motif in RelB. *J. Mol. Biol. 394*, 183-196.

(32) Wang, X. X., and Wood, T. K. (2011) Toxin-antitoxin systems influence biofilm and persister cell formation and the general stress response. *Appl. Environ. Microbiol. 77*, 5577-5583.

(33) Kwan, B. W., Lord, D. M., Peti, W., Page, R., Benedik, M. J., and Wood, T. K. (2015) The MqsR/MqsA toxin/antitoxin system protects *Escherichia coli* during bile acid stress. *Environ. Microbiol. 17*, 3168–3181.

(34) Janssen, B. D., Garza-Sánchez, F., and Hayes, C. S. (2015) YoeB toxin is activated during thermal stress. *Microbiologyopen 4*, 682-697.

(35) Elowitz, M. B., Levine, A. J., Siggia, E. D., and Swain, P. S. (2002) Stochastic gene expression in a single cell. *Science 297*, 1183-1186.

(36) Van den Bergh, B., Fauvart, M., and Michiels, J. (2017) Formation, physiology, ecology, evolution and clinical importance of bacterial persisters. *FEMS Microbiol. Rev. 41*, 219-251.

(37) Fasani, R. A., and Savageau, M. A. (2013) Molecular mechanisms of multiple toxin-antitoxin systems are coordinated to govern the persister phenotype. *Proc. Natl. Acad. Sci. U. S. A. 110*, E2528-E2537.